Shared NADPH regeneration sets sharp limits on joint glutathione and thioredoxin service

16 September 2026

Abstract

Two antioxidant branches that operate adequately in separate preparations need not meet the same branch-resolved requirements when they are coupled to a single NADPH regeneration system. We study a maintained-peroxide subsystem of published redox kinetics that retains finite enzyme and carrier inventories, including enzyme-bound glutathione. Exact elimination of the private states gives, for each branch, a positive quadratic carrier response and a strictly increasing service current as a function of the shared NADPH concentration. Against a strictly decreasing regeneration current this yields a necessary and sufficient condition for joint service, an explicit and attained minimum regeneration capacity, a reconstruction of every steady-state species, and uniqueness of the full joint steady state. We prove that a finite regeneration repair exists exactly when each quota lies strictly below its branch ceiling current, and we identify the exact deficit of a quota-only capacity estimate as kinetic overdelivery. For declared nominal parameters and design quotas of 10 and 4 $\mu\mathrm{M\,s^{-1}}$, both isolated preparations succeed while their joint preparation fails at one tenth of the reference regeneration capacity; the attained minimum requires a certified 13.71266–13.71268% increase over that setting. Allowing one enzyme inventory to change attains the quota-only bound exactly, with a 3.3727% reduction in the glutathione peroxidase pool, and we prove a matching lower bound over every admitted redesign of that branch. The decision criterion, the separate-preparation comparison, the uniqueness and ceiling theorems and the constructive redesign are checked in Lean 4. We also delimit the result: we give the exact interval criterion that replaces the threshold when branch service is not monotone, an explicit analytic example in which excess regeneration destroys service without bistability, and a sign obstruction showing that the eight-variable kinetics admit no orthant order making them cooperative near the boundary equilibrium. The result concerns kinetic service in a declared maintained system. It is not a claim about whole-cell protection, clinical benefit, or thermodynamic incompatibility.

1 Introduction

Shared reducing power couples reactions that can each look adequate in isolation. Glutathione peroxidase and the peroxiredoxin–thioredoxin system both clear hydrogen peroxide, and both are ultimately restored by NADPH through their own reductases [10, 14, 18]. A design question that arises whenever such branches are assembled into one preparation is therefore not merely whether each branch has sufficient enzyme, but whether the service each branch is required to deliver can coexist with the other at one physically shared NADPH concentration.

Answering that question requires actual kinetic demand rather than an assigned flux. A branch can consume more reducing power than its specified minimum service, and deleting its requirement does not delete that consumption. This distinction is the whole content of the difference between the two capacity numbers computed below, and it is not an artefact of a particular numerical solver.

Adimora et al. [2] developed a coupled model of cellular hydrogen peroxide responses that includes glutathione, thioredoxin, peroxiredoxin, protein thiols and catalase. The present

contribution is not the introduction of that biochemical coupling, nor a new calibration of it. It is an exact decision and reconstruction theorem for a specified maintained subnetwork of those kinetics. The proof retains the private enzyme and carrier states before eliminating them at steady state, and identifies precisely which scalar boundary determines joint operation.

Results. Let x denote the shared NADPH concentration. After exact elimination, each branch i has a carrier $u_i(x)$ solving a quadratic with a single positive root and a service current $j_i(x)$ that is a strictly increasing rational function of u_i (Propositions 3.1 and 3.3). A quota $j_i \geq q_i$ is therefore equivalent to an explicit NADPH floor $x \geq X_i$. Against the strictly decreasing regeneration current this gives:

- a necessary and sufficient criterion for joint service, with an attained minimum regeneration scale $s_{\min} = J(L)/R_1(L)$ at $L = \max_i X_i$ (Theorem 3.4);
- uniqueness of the full joint steady state, in every private enzyme and carrier coordinate, not only in x (Theorem 3.5);
- an exact identity for the deficit of the quota-only capacity estimate, namely total kinetic overdelivery at the binding floor (Proposition 4.1);
- an equivalence for repairability: some finite regeneration scale works if and only if $q_i < j_i(N)$ for both branches, where N is the largest admissible NADPH concentration (Theorem 4.2);
- a constructive change of one enzyme inventory that attains the quota-only bound, together with a matching lower bound over all admitted redesigns of that branch (Section 5).

Sections 7 and 8 delimit the result rather than extend it. We record which hypotheses the criterion actually needs, what replaces it when branch service is not monotone, and exactly what the numerical dynamics do and do not establish.

What is claimed and what is not. Every theorem below is a statement about a declared kinetic system with fixed peroxide, conserved carrier inventories and an externally maintained regeneration drive. The service quotas are independently specified design requirements; they are not measured health thresholds, and we translate them into reduced-carrier floors so that this is visible. Nothing here establishes whole-cell protection, a clinical intervention, a thermodynamic impossibility, or global attraction of the full kinetics. The formal verification described in Appendix C establishes that the stated propositions follow from their stated hypotheses in Lean's kernel; it does not validate the choice of equations, the transcription of the source model, or any biological interpretation.

Organization. Section 2 states the maintained model and what service means. Section 3 gives the elimination, the criterion and uniqueness. Section 4 derives design consequences, and Section 5 the optimal enzyme reallocation. Section 6 works the nominal preparation. Section 7 determines how far the criterion extends, Section 8 treats the full dynamics, and Section 9 compares with existing methods and describes a discriminating experiment. Appendix A gives the full ODE and the numerical protocol, Appendix B a conservative parameter-box bound, and Appendix C the formal-verification scope and declaration map.

2 The maintained model

All concentrations are in μM and time in seconds. The peroxide concentration H is externally fixed, so that the peroxide-dependent rate constants below are constants of the maintained preparation.

2.1 Shared pyridine pool and regeneration

Write x for NADPH and $P - x$ for $NADP^+$, where the pyridine total P is conserved, and write P_0 for the baseline oxidized concentration retained by the source model's regeneration law. With

$$N = P - P_0, \qquad D = K + P,$$

regeneration is

$$R_s(x) = sV\,\frac{N - x}{D - x} = s\,R_1(x), \qquad 0 < x \le N < D, \quad s, V > 0. \tag{1}$$

Here V is a reference capacity, $s > 0$ is a dimensionless regeneration scale, and the product sV is a *capacity* parameter. The realized regeneration current is $R_s(x)$, which is strictly smaller than sV throughout the physical range; we keep this distinction in every table and figure. The substrate and energy supply driving this source are maintained, not modelled as a finite reservoir.

Two structural facts about (1) are all that the argument uses: R_s is strictly decreasing on $[0, N]$, and $R_s(N) = 0$. Section 7.1 records the corresponding general statement.

2.2 Glutathione branch

Let g and z denote free GSH and GSSG, and let e_0, e_1, e_2 denote reduced GPx, oxidized GPx and the GPx–SSG intermediate. With branch-specific positive constants a_G, b_G, c_G, k_G the four currents are

$$a_G e_0, \qquad b_G\, g\, e_1, \qquad c_G\, g\, e_2, \qquad k_G\, x\, (z - z_{G0}), \tag{2}$$

the last being the baseline-corrected glutathione reductase law. The maintained peroxide concentration is absorbed into a_G. At steady state all four currents equal a common value j_G. The conservation laws are

$$e_0 + e_1 + e_2 = E_G, \qquad g + 2z + e_2 = G. \tag{3}$$

The final term of the second law counts the glutathione bound in the enzyme intermediate. Omitting it gives a different model and a different decision boundary, even when the intermediate's concentration is numerically small.

2.3 Peroxiredoxin–thioredoxin branch

Let y and z_T denote reduced and oxidized Trx, with $y + z_T = T$, and let r, h, w, v denote reduced, sulfenic, hyperoxidized and disulfide Prx. The transitions are

$$r \xrightarrow{a_T} h, \qquad h \xrightarrow{b_T} w, \qquad w \xrightarrow{c_T} h, \qquad h \xrightarrow{d_T} v, \qquad v \xrightarrow{e_T y} r. \tag{4}$$

The peroxide concentration is absorbed into a_T and b_T. The transition $w \to h$ returns hyperoxidized to sulfenic Prx; it is retained exactly as the source model's first-order phenomenological maintenance law. The model does not resolve its energetic or reducing inputs, which in biological sulfiredoxin repair include ATP and a thiol reductant [9]; we therefore keep it visible as an external input throughout (Table 4). Thioredoxin regeneration is $k_T\, x\, (z_T - z_{T0})$. At steady state,

$$a_T r = d_T h = e_T y v = k_T x (z_T - z_{T0}) = j_T, \qquad c_T w = b_T h, \qquad r + h + w + v = E_T. \tag{5}$$

All rate constants are positive except that $b_T \ge 0$ is allowed, and the baselines z_{G0}, z_{T0} are nonnegative.

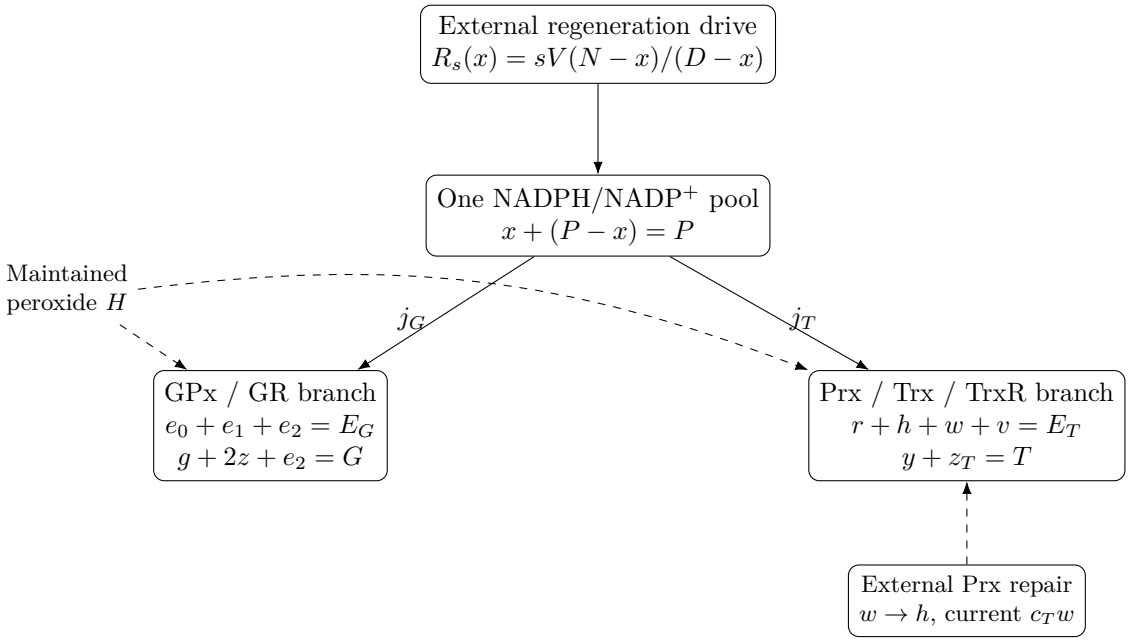

Figure 1: Physical ownership in the maintained preparation. The two branches keep private carrier and enzyme inventories but draw on one NADPH regeneration balance. Dashed arrows denote externally maintained inputs. The Prx repair input lies outside the counted NADPH currents, and the peroxide clamp is an experimental assumption rather than a finite bolus.

2.4 Ownership, service and observables

The branches share the variable x and one balance,

$$R_s(x) = j_G + j_T, \tag{6}$$

and nothing else: enzyme pools, carrier pools and baselines are private (Figure 1).

Definition 2.1 (Joint service)**.** Given quotas $q_G, q_T > 0$, *joint service at scale* s means the existence of a steady state of the full system with $0 < x \leq N$, all private concentrations positive (with $w = 0$ permitted exactly when $b_T = 0$), satisfying (3), (5), (6) and $j_G \geq q_G$, $j_T \geq q_T$.

The quotas are independently specified assay requirements. Section 7.3 translates them into equivalent reduced-carrier floors, which is the form in which they are measurable; they are not measured health thresholds. Two operations that are often conflated must be separated at the outset:

- A *separate preparation* physically removes the other branch, and with it that branch's demand: the removed term disappears from (6).
- *Relaxing a quota* removes only an inequality. Both terms remain in (6), and the removed branch's kinetic consumption is unchanged.

Peroxide removal is a different observable from NADPH consumption. At steady state GPx removes peroxide at rate j_G, while Prx removes it at $a_T r + b_T h = j_T(1 + b_T/d_T)$, so the maintained peroxide influx that this selected subsystem requires is

$$I_H = j_G + j_T + \frac{b_T}{d_T}\, j_T, \tag{7}$$

where the last contribution is accompanied by the external repair current $c_T w$. Counted NADPH consumption is $j_G + j_T$. No omitted pathway is silently included in either observable.

Away from equilibrium the peroxide sink is instead $a_G e_0 + a_T r + b_T h$ and the instantaneous source demand is $k_G x(z - z_{G0}) + k_T x(z_T - z_{T0})$; these coincide with the branch service currents only at steady state.

3 Exact elimination and the joint boundary

Set

$$\rho_G = a_G\left(\frac{1}{b_G} + \frac{1}{c_G}\right), \quad S_G = G - 2z_{G0}, \qquad \rho_T = \frac{1}{a_T} + \frac{1}{d_T} + \frac{b_T}{c_T d_T}, \quad S_T = T - z_{T0}, \tag{8}$$

and assume throughout the *positive-pool conditions*

$$S_G\rho_G > \frac{E_G a_G}{c_G}, \qquad S_T > 0. \tag{9}$$

These are model assumptions supporting the positive-root construction, not measured physiological laws. The first says that the available glutathione exceeds a limiting enzyme-bound inventory; it holds comfortably for the nominal values of Section 6, where its two sides are 1923.915 and 1.05 $\mu\mathrm{M}^2$.

3.1 Private-state elimination

Proposition 3.1 (Private-state elimination)**.** *Assume* (9)*. For each $x > 0$ the private steady states are in bijection with the positive roots of*

$$g^2 + \left(\rho_G - S_G + \frac{2E_G a_G}{k_G x}\right) g - \left(S_G\rho_G - \frac{E_G a_G}{c_G}\right) = 0, \tag{10}$$

$$\rho_T e_T\, y^2 + \left(1 - S_T\rho_T e_T + \frac{E_T e_T}{k_T x}\right) y - S_T = 0, \tag{11}$$

each of which has exactly one positive root. The corresponding currents are

$$j_G(x) = \frac{E_G a_G\, g(x)}{g(x) + \rho_G}, \qquad j_T(x) = \frac{E_T e_T\, y(x)}{1 + \rho_T e_T\, y(x)}, \tag{12}$$

and every private species is reconstructed from them by

$$(e_0, e_1, e_2, z) = \left(\frac{j_G}{a_G},\ \frac{j_G}{b_G g},\ \frac{j_G}{c_G g},\ z_{G0} + \frac{j_G}{k_G x}\right), \tag{13}$$

$$(r, h, w, v, z_T) = \left(\frac{j_T}{a_T},\ \frac{j_T}{d_T},\ \frac{b_T j_T}{c_T d_T},\ \frac{j_T}{e_T y},\ z_{T0} + \frac{j_T}{k_T x}\right). \tag{14}$$

Proof. Equating the four glutathione currents in (2) to their common steady value j_G gives (13). Substituting into the enzyme sum in (3) gives $j_G(1/a_G + 1/(b_G g) + 1/(c_G g)) = E_G$, that is, the first expression in (12). Substituting (13) and (12) into $g + 2z + e_2 = G$ and multiplying by $g + \rho_G > 0$ gives (10). Every division performed has a strictly positive denominator on the admitted domain, so each step is reversible: a positive root of (10) reconstructs a positive private state satisfying all four current equalities and both conservation laws.

For the second branch, (5) gives (14), and the Prx sum becomes $j_T(\rho_T + 1/(e_T y)) = E_T$, which is the second expression in (12). The Trx conservation law then gives (11). The reconstruction also verifies the sulfenic balance $a_T r + c_T w - (b_T + d_T)h = 0$ and the hyperoxidation balance $c_T w = b_T h$.

Each polynomial has positive leading coefficient, and by (9) a strictly negative constant term, so it has exactly one positive root. □

Both branches therefore have the common form

$$A_i\,u_i^2 + \left(B_i + \frac{C_i}{x}\right) u_i - \Gamma_i = 0, \qquad j_i(x) = \frac{p_i\,u_i(x)}{v_i\,u_i(x) + w_i}, \tag{15}$$

with $A_i, C_i, \Gamma_i, p_i, w_i > 0$ and $v_i \geq 0$, the sign of B_i being unrestricted. Writing $u_G = g$ and $u_T = y$, the coefficients are read off from (10)–(12):

	A_i	B_i	C_i	Γ_i	p_i	v_i	w_i
GPx, $u_G = g$	1	$\rho_G - S_G$	$\dfrac{2E_G a_G}{k_G}$	$S_G\rho_G - \dfrac{E_G a_G}{c_G}$	$E_G a_G$	1	ρ_G
Trx, $u_T = y$	$\rho_T e_T$	$1 - S_T\rho_T e_T$	$\dfrac{E_T e_T}{k_T}$	S_T	$E_T e_T$	$\rho_T e_T$	1

The constant Γ_i of (15) is a branch quantity, distinct from the source parameter D of (1); we use different symbols throughout to avoid the collision.

Remark 3.2 (Numerically stable evaluation). With $\beta = B_i + C_i/x$ the positive root of (15) is

$$u_i = \begin{cases} \dfrac{2\Gamma_i}{\beta + \sqrt{\beta^2 + 4A_i\Gamma_i}}, & \beta \geq 0, \\[2ex] \dfrac{-\beta + \sqrt{\beta^2 + 4A_i\Gamma_i}}{2A_i}, & \beta < 0. \end{cases}$$

The two branches of this formula avoid cancellation for small x, where β is large and positive. This affects floating-point evaluation only, not the mathematical root; all exact statements below use the root itself.

3.2 Threshold inversion

Proposition 3.3 (Threshold inversion)**.** *For each branch, u_i and j_i are continuous and strictly increasing on $x > 0$, and*

$$u_i'(x) = \frac{C_i\,u_i}{x^2(2A_i u_i + B_i + C_i/x)} > 0, \qquad \frac{\mathrm{d}j_i}{\mathrm{d}u_i} = \frac{p_i w_i}{(v_i u_i + w_i)^2} > 0. \tag{16}$$

Given a quota $q_i > 0$, define

$$Y_i = \frac{q_i w_i}{p_i - q_i v_i}, \qquad \Delta_i = \Gamma_i - A_i Y_i^2 - B_i Y_i, \qquad X_i = \frac{C_i Y_i}{\Delta_i}. \tag{17}$$

If $p_i - q_i v_i > 0$ and $\Delta_i > 0$, then for every $x > 0$

$$j_i(x) \geq q_i \iff u_i(x) \geq Y_i \iff x \geq X_i, \qquad \text{and} \qquad j_i(X_i) = q_i. \tag{18}$$

Proof. The root is $[-\beta + \sqrt{\beta^2 + 4A_i\Gamma_i}]/(2A_i)$ with $\beta = B_i + C_i/x$, which is continuous in $x > 0$; the stated derivative follows by implicit differentiation, the bracket in its denominator being $\sqrt{\beta^2 + 4A_i\Gamma_i} > 0$. Increasing x strictly decreases the left side of (15) at every positive argument; since that expression is negative below its positive root and positive above it, the root strictly increases. The derivative of the rational current in u_i is as stated and is positive.

For the inversion, solving $q_i \leq p_i u/(v_i u + w_i)$ for u gives $u \geq Y_i$ under $p_i - q_i v_i > 0$. Evaluating the left side of (15) at $u = Y_i$ gives $-\Delta_i + C_i Y_i/x$, which is nonpositive exactly when $x \geq C_i Y_i/\Delta_i = X_i$; since the expression is nonpositive at Y_i precisely when $Y_i \leq u_i(x)$, this is the second equivalence. Equality at $x = X_i$ gives $u_i(X_i) = Y_i$ and hence $j_i(X_i) = q_i$. □

The formal development establishes continuity, strict monotonicity and the inversion (18) directly, without the explicit derivative formulas; the first of those is recorded here only because it is used again in (24).

3.3 The sharp criterion

Theorem 3.4 (Sharp joint regeneration criterion)**.** *Assume the positive-pool conditions (9), the quota conditions of Proposition 3.3 for both branches, and*

$$L := \max(X_G, X_T) < N < D, \qquad V > 0.$$

Write $J(x) = j_G(x) + j_T(x)$ *and*

$$s_{\min} = \frac{J(L)}{R_1(L)} = \frac{J(L)\,(D-L)}{V\,(N-L)}. \tag{19}$$

Then for every $s > 0$*, joint service at scale* s *in the sense of Definition 2.1 holds if and only if* $s \geq s_{\min}$*. At* $s = s_{\min}$ *the steady state has* $x = L$ *and the private states (13)–(14); the minimum is attained, not merely an infimum.*

Proof. By Proposition 3.3 both quotas hold exactly when $x \geq L$. On $[L, N]$ put $F_s(x) = R_s(x) - J(x)$. This is continuous, and strictly decreasing because J is strictly increasing while $R_s'(x) = -sV(D-N)/(D-x)^2 < 0$. At the right endpoint $R_s(N) = 0$, so $F_s(N) = -J(N) < 0$. Hence F_s has a zero in $[L, N]$ if and only if $F_s(L) \geq 0$, by the intermediate value theorem, and that zero is then unique in $[L, N]$. Since $R_1(L) > 0$ and $R_s(L) = sR_1(L)$, the condition $F_s(L) \geq 0$ is exactly $s \geq J(L)/R_1(L) = s_{\min}$.

A zero $x^\star$ of F_s in $[L, N]$ satisfies both quotas and the shared balance, and Proposition 3.1 reconstructs from it a full steady state with all private concentrations positive. Conversely, any full steady state meeting both quotas has $x \geq L$ and zero shared residual, hence is such a zero. At $s = s_{\min}$ we have $F_s(L) = 0$, so the zero is L itself. □

Theorem 3.5 (Uniqueness of the joint steady state)**.** *Under the hypotheses of Theorem 3.4, any two full steady states meeting both quotas at the same scale* s *have the same NADPH concentration and the same value of every private enzyme and carrier variable:* $x = x'$*,* $(g, z, e_0, e_1, e_2) = (g', z', e_0', e_1', e_2')$ *and* $(y, z_T, r, h, w, v) = (y', z_T', r', h', w', v')$*.*

Proof. By Proposition 3.1 each witness has its carriers equal to the unique positive roots at its own x, hence its currents equal $j_G(x)$ and $j_T(x)$; by Proposition 3.3 both quotas force $x \geq L$. Both witnesses therefore lie in $[L, N]$ and are zeros of the same strictly decreasing function F_s, so $x = x'$. Given $x = x'$, the carrier values agree because the positive root is unique, so the currents agree, and each remaining species is then determined by dividing that common current by a strictly positive constant in (13)–(14). □

Uniqueness in the full state, rather than in the scalar x alone, is what licenses reporting a single reconstructed species table for the boundary preparation (Table 3).

3.4 What the theorem does not say

Theorem 3.4 is a statement about steady states. It does not assert that transient trajectories lie on the scalar response curve $x \mapsto J(x)$: away from equilibrium the private states are not slaved to x, and the instantaneous reductase currents differ from the branch service currents. It gives no rate of approach and no basin of attraction; Section 8 says what is and is not known about those questions.

Below $s_{\min}$ a positive steady state still exists; it simply fails at least one quota. Indeed, as $x \downarrow 0$ the positive root of (15) satisfies $0 < u_i \leq \Gamma_i/(B_i + C_i/x) \to 0$, so $J(x) \to 0$, while $R_s(0) = sVN/D > 0$; combined with $F_s(N) < 0$ and strict monotonicity this gives a unique positive equilibrium on $(0, N)$ for every $s > 0$. Failure below $s_{\min}$ is therefore failure of the service requirements, not loss of a steady state.

4 Consequences for design

4.1 Separate preparations and kinetic overdelivery

With the other branch physically absent, the same argument applied to a single branch gives the isolated requirement

$$s_i^{\text{isolated}} = \frac{j_i(X_i)}{R_1(X_i)} = \frac{q_i}{R_1(X_i)}. \tag{20}$$

Each separate preparation has access to its own full source setting, which is why both can succeed at a scale where the joint preparation fails. Comparing branch currents between preparations is meaningful only once this is stated.

A natural first estimate of the joint requirement replaces actual demand by the quotas,

$$s_{\text{quota}} = \frac{q_G + q_T}{R_1(L)}.$$

The following identity says exactly what that estimate omits.

Proposition 4.1 (Overdelivery identity)**.** *Under the hypotheses of Theorem 3.4,*

$$s_{\min} - s_{\text{quota}} = \frac{[j_G(L) - q_G] + [j_T(L) - q_T]}{R_1(L)} \;\geq\; 0, \tag{21}$$

with equality if and only if both currents equal their quotas at L, that is, if and only if $X_G = X_T$.

Proof. The identity is immediate from (19). Both numerator terms are nonnegative because $x = L$ satisfies both quotas, so their sum vanishes exactly when each vanishes; by (18) $j_i(L) = q_i$ holds exactly when $L = X_i$, and $L = \max(X_G, X_T)$. □

The gap is therefore *kinetic overdelivery*: at the binding floor the non-binding branch delivers strictly more than it was asked for, and that excess consumes NADPH. Two readings must be kept apart. Relative to the stated pair of requirements, the excess is capacity overhead. It is not waste in any biological sense, since the extra peroxide clearance is real; Section 6 quantifies both statements for the nominal preparation.

4.2 Repairability and the finite-source ceiling

Increasing regeneration cannot raise a branch current above its value at $x = N$. The next theorem turns that observation into an exact criterion for the existence of *any* finite repair.

Theorem 4.2 (Finite-source ceiling)**.** *Fix admitted branch kinetics with (9), positive quotas q_G, q_T, and $0 < N < D$. Then some finite scale $s > 0$ admits joint service if and only if*

$$q_G < j_G(N) \qquad \textit{and} \qquad q_T < j_T(N). \tag{22}$$

Proof. Necessity. At a steady state with positive currents, $x = N$ is impossible because regeneration vanishes there while demand does not; hence $x < N$, and strict monotonicity gives $q_i \leq j_i(x) < j_i(N)$.

Sufficiency. Suppose $q_i < j_i(N)$. Writing $u_N = u_i(N)$, the inequality $q_i < p_i u_N/(v_i u_N + w_i)$ gives $p_i - q_i v_i > 0$ and $Y_i < u_N$. Since the left side of (15) at $x = N$ is negative below its root, evaluating it at Y_i gives $C_i Y_i/N < \Delta_i$; in particular $\Delta_i > 0$, so the quota conditions of Proposition 3.3 hold, and the same inequality rearranges to $X_i = C_i Y_i/\Delta_i < N$. Thus $L = \max(X_G, X_T) < N$, all hypotheses of Theorem 3.4 hold, and $s = s_{\min}$ is a finite admissible scale. □

So a quota at or above its branch ceiling cannot be met by any amount of regeneration: the obstruction is the finite carrier and enzyme inventory, not the source. The cost of operating near a ceiling is quantified by the following limit, in which the kinetics are held fixed and only the binding floor is moved.

Corollary 4.3 (Near-ceiling cost)**.** *With branch kinetics fixed and $L \uparrow N$,*

$$s_{\min}(L) \;\sim\; \frac{J(N)\,(D-N)}{V\,(N-L)}. \tag{23}$$

Proof. Divide (19) by the right side of (23): the ratio is $J(L)(D-L)/\big[J(N)(D-N)\big]$, which tends to 1 by continuity, the denominator being positive. □

4.3 The binding-quota plateau and the cost of a stricter requirement

Only the larger threshold controls the repair. If $X_G \le X_T$ then changing q_G in any way that keeps its threshold at most X_T leaves L, and hence $s_{\min}$, unchanged. In particular, lowering a non-binding quota does not lower that branch's kinetic consumption, and does not reduce the required capacity at all. The quota-only estimate does decrease, which is precisely why it is not a valid capacity bound.

For a uniquely binding branch the local cost of a stricter requirement is explicit. Writing $h(x) = J(x)/R_1(x)$, which is strictly increasing because $J' > 0 > R_1'$, the binding branch k satisfies

$$\frac{\partial s_{\min}}{\partial q_k} = \frac{h'(X_k)}{j_k'(X_k)}, \qquad \frac{\partial s_{\min}}{\partial q_{k'}} = 0 \;\text{ for the non-binding branch,} \tag{24}$$

with one-sided derivatives at a tie, where the maximum of the two thresholds may have a corner. Equation (24) follows from $s_{\min} = h(X_k)$ and $\mathrm{d}X_k/\,\mathrm{d}q_k = 1/j_k'(X_k)$, the latter by differentiating $j_k(X_k) = q_k$. At the nominal parameters of Section 6 its value is 0.009912 per $\mu\mathrm{M\,s^{-1}}$ of Trx quota.

4.4 Regeneration tolerance

Suppose the realized scale differs multiplicatively from the commanded one,

$$s_{\text{actual}} = \eta\, s_{\text{command}}, \qquad \eta \in [1-\epsilon, 1+\epsilon], \quad 0 \le \epsilon < 1.$$

Then joint service for every admissible η holds if and only if

$$s_{\text{command}} \;\ge\; \frac{s_{\min}}{1-\epsilon}, \tag{25}$$

since the smallest realized scale is $(1-\epsilon)s_{\text{command}}$ and Theorem 3.4 applies to it. This is a statement about a family of constant settings. Arbitrarily time-varying fluctuations require a dynamical argument, and (25) alone does not establish transient quota preservation. The tolerance ϵ is an assumed engineering specification, not a biological confidence interval; Appendix B treats parameter uncertainty separately and conservatively.

5 A constructive and optimal enzyme reallocation

The criterion separates three interventions that are easily conflated: relaxing a requirement, changing an enzyme inventory, and increasing regeneration. Only the last two change the kinetics or the operating point. We now show that the second can remove the overdelivery gap of Proposition 4.1 entirely, and that it cannot do better.

Keep the Trx branch, all rate constants and both conserved carrier totals fixed, and allow the GPx inventory E_G to vary. Suppose $X_G \le X_T$, so that the Trx branch binds, and aim at the operating point $x = X_T$ with j_G exactly at quota. Then $e_2 = q_G/(c_G g)$ and $z = z_{G0} + q_G/(k_G X_T)$, so glutathione conservation reads $g + 2q_G/(k_G X_T) + q_G/(c_G g) = S_G$, that is,

$$g^2 - \left(S_G - \frac{2q_G}{k_G X_T}\right) g + \frac{q_G}{c_G} = 0, \qquad E_G^\star = \frac{q_G\,(g + \rho_G)}{a_G\, g}. \tag{26}$$

Proposition 5.1 (Attainment)**.** *Suppose* (26) *has a positive root* $g^\star$ *for which the reconstructed state is admissible, that is,* $E_G^\star > 0$ *and the redesigned branch satisfies* (9)*. Then the preparation with inventory* $E_G^\star$ *achieves both quotas exactly at* $x = X_T$*, at the scale*

$$s^\star = \frac{q_G + q_T}{R_1(X_T)} = s_{\text{quota}}. \tag{27}$$

Proof. By construction the reconstructed glutathione state satisfies every current equality and both conservation laws with $j_G = q_G$, and the unchanged Trx branch at $x = X_T$ has $j_T = q_T$ by (18). The shared balance (6) then reads $sR_1(X_T) = q_G + q_T$, giving (27). □

Admissibility is a genuine side condition: it requires a nonnegative discriminant in (26), a positive reconstructed state, and the positive-pool condition for the *new* inventory. It must be checked, not inferred from the quadratic alone. When two positive roots exist, $E_G^\star$ in (26) is decreasing in g, so the larger root uses the smaller enzyme pool at this fixed x and quota.

Proposition 5.2 (Matching lower bound)**.** *Let the Trx branch and all carrier totals be fixed with* X_T *binding. Then every admitted glutathione branch — in particular every choice of* E_G *— that achieves joint service at some scale* s *requires* $s \ge s^\star$*.*

Proof. Any successful preparation must satisfy the unchanged Trx quota, so its operating point has $x \ge X_T$ by (18). Its shared balance and the two quotas give $q_G + q_T \le j_G + j_T = sR_1(x)$. Since R_1 is strictly decreasing and $x \ge X_T$, this yields $q_G + q_T \le sR_1(X_T)$, which is $s \ge s^\star$. □

Propositions 5.1 and 5.2 together say that changing one enzyme inventory attains exactly the quota-only bound and nothing better: the reallocation can remove the overdelivery overhead, but it cannot evade the requirement that both quotas be delivered at an NADPH concentration at least X_T. The conclusion is narrow. It states that a controlled change of a declared enzyme inventory reduces the regeneration capacity needed for a specified pair of branch-resolved services in a maintained preparation. It is not a global minimization of protein cost, not a statement about a different peroxide load, and emphatically not a recommendation to inhibit GPx in a cell.

6 The nominal preparation

The parameter assignments in Table 1 are inherited from the published model [2], which itself combines measurements with literature-derived effective kinetics obtained under heterogeneous conditions. They are not a new homogeneous enzyme calibration, and we do not upgrade their provenance here. The lower block of the table lists the quantities that are design choices of the present study. The source model's negligible assigned initial intermediates are omitted from the declared exact totals; the bound intermediate e_2 is fully retained thereafter, inside the glutathione inventory.

Table 1: Declared coefficients and inventories. Concentrations are in μM; unimolecular rates in s^{-1} and bimolecular rates in $\mu M^{-1}s^{-1}$. The constants a_G, a_T, b_T absorb the maintained peroxide concentration H. Source reaction labels refer to the tables of Adimora et al. [2].

Quantity	Value	Origin and role
P, P_0, K, V	30.3, 0.3, 57, 375	Source pool and regeneration law (R7, R22)
N, D	30, 87.3	Derived: $N = P - P_0$, $D = K + P$
G, z_{G0}, E_G	371.56, 1.78, 50	Declared source-derived glutathione and GPx pools
T, z_{T0}, E_T	0.505, 0.075, 19.096	Declared source-derived Trx and Prx pools
a_G, b_G, c_G, k_G	0.21, 0.04, 10, 3.2	Source reactions R3–R5, R20
a_T, b_T, c_T	0.4, 0.00072, 0.003	Source reactions R8–R10
d_T, e_T, k_T	15, 2.1, 20	Source reactions R11–R12, R21
H	0.01	Maintained peroxide challenge: design choice
s_0	0.1	Reference regeneration setting: design choice
q_G, q_T	10, 4	Branch service requirements: design choices

6.1 Thresholds, the binding branch and the attained minimum

With these values, (17) gives exact rational thresholds

$$X_G = \frac{3294375}{138400918} \approx 0.0238031297, \qquad X_T = \frac{460180}{489387} \approx 0.9403192157 \quad (\mu\text{M}),$$

so the thioredoxin branch binds and $L = X_T$. At $x = L$ the carriers are $g \approx 361.1185236$ μM and $y = 5000/23009 \approx 0.2173062715$ μM, and the currents are

$$j_G(L) = 10.348943552 \ \mu\text{M}\,\text{s}^{-1}, \qquad j_T(L) = 4 \ \mu\text{M}\,\text{s}^{-1}.$$

The Trx quota is therefore equivalent to the reduced-carrier floor $y \geq 5000/23009$, which is 43.03% of the total Trx pool T and 50.54% of the maximum reduced amount $S_T = 0.43$ μM permitted by the baseline offset. This is a measurable model endpoint, not an authenticated health threshold, and the denominator must be stated with it.

The minimum scale is enclosed by exact rational arithmetic,

$$0.11371266 \ \leq \ s_{\min} \ \leq \ 0.11371268, \tag{28}$$

with numerical value 0.113712668. Relative to the reference setting $s_0 = 0.1$ this is a certified 13.71266–13.71268% increase, and the corresponding capacity $s_{\min}V$ lies between 42.6422475 and 42.642255 $\mu\text{M}\,\text{s}^{-1}$. The width of (28) reflects mathematical enclosure, not biological uncertainty. The realized boundary demand is $J(L) = 14.348943552$ $\mu\text{M}\,\text{s}^{-1}$, which should not be confused with the capacity $s_{\min}V = 42.642250$ $\mu\text{M}\,\text{s}^{-1}$.

6.2 Separate success and joint failure

At the reference setting $s_0 = 0.1$ the two isolated preparations deliver 10.351411 and 5.129763 $\mu\text{M}\,\text{s}^{-1}$, both above their quotas; their individual requirements are only $s = 0.077641$ and $s = 0.031699$. The joint preparation at the same setting equilibrates at $x \approx 0.3597903$ μM with currents 10.344228 and 2.440510 $\mu\text{M}\,\text{s}^{-1}$, so the Trx quota fails by a wide margin (Figure 2). Both isolated successes and the joint failure are verified in Lean.

Joint quota failure is not a statement that adding the second branch lowered aggregate antioxidant activity. At that same setting the total counted NADPH turnover is $j_G + j_T \approx 12.784739$ $\mu\text{M}\,\text{s}^{-1}$, already larger than the GPx-only current 10.351411 $\mu\text{M}\,\text{s}^{-1}$, and the peroxide turnover (7) is larger still. What fails is the specified pair of branch-resolved requirements.

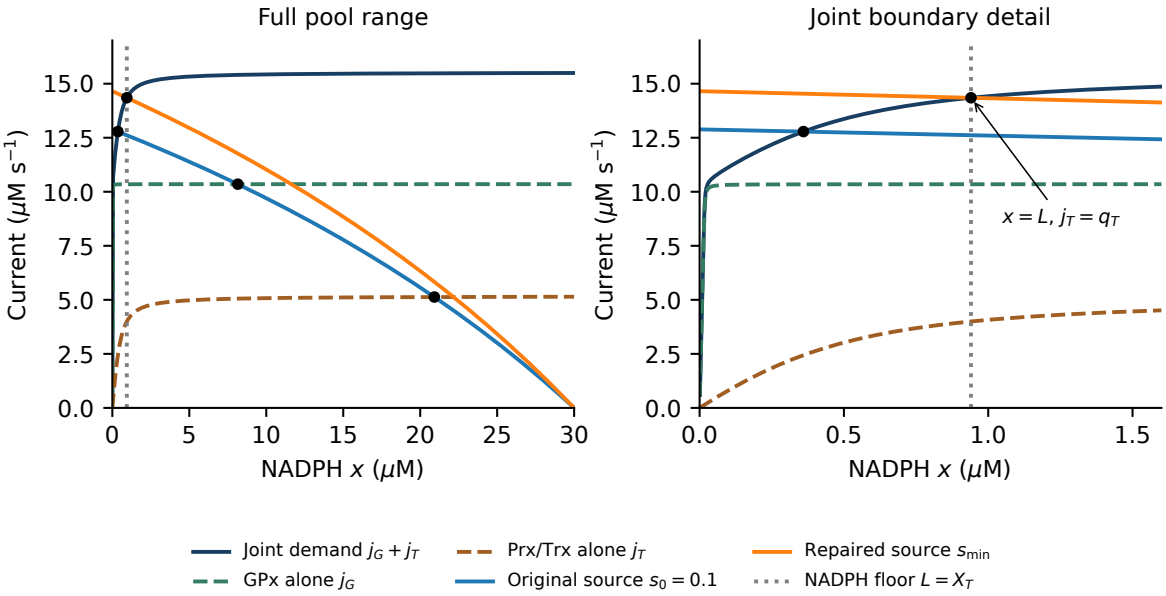

Figure 2: The same kinetic laws in separate and joint preparations. Intersections of a source curve with a demand curve determine the equilibrium NADPH concentration; black markers show the isolated GPx, isolated Prx/Trx and joint equilibria at $s_0 = 0.1$, and the joint equilibrium at $s_{\min}$. The repaired source meets the joint demand exactly at the binding floor $L = X_T$, where the Trx current equals its quota. Direct numerical solution of these same kinetics reproduces the boundary; the theorem adds necessity, sufficiency, attainment and species reconstruction.

6.3 Repair decisions and the overdelivery penalty

Table 2 collects the capacity decisions. The kinetic overdelivery of Proposition 4.1 is $j_G(L) - q_G = 0.348943552\ \mu\mathrm{M\,s^{-1}}$, entirely on the non-binding GPx branch. It makes the true requirement 2.49245% larger than the quota-only estimate; as repair percentages relative to s_0, the two differ by 2.76531 percentage points. This is an identified kinetic effect with a closed-form value, not an unexplained discrepancy between two numerical procedures.

The redesign of Section 5 takes the larger root of (26), $g^\star \approx 361.3505536\ \mu$M, giving

$$E_G^\star \approx 48.313664\ \mu\mathrm{M},$$

a 3.37267% reduction of the GPx pool. Both currents then sit exactly at quota and the quota-only bound is attained. The smaller root of (26) is rejected: it would require an enzyme

Table 2: Repair decisions for the declared preparation. Capacity is sV, not realized steady flux; the realized demand at the boundary is $14.348944\ \mu\mathrm{M\,s^{-1}}$. Decimal entries are numerical evaluations of exact quantities, except that the fixed-kinetics minimum is additionally enclosed by (28).

Decision	Scale s	Capacity sV ($\mu\mathrm{M\,s^{-1}}$)	Change from s_0
Reference preparation	0.100000000	37.500000	0%
Quota-only bound	0.110947356	41.605259	10.947356%
Fixed-kinetics minimum $s_{\min}$	0.113712668	42.642250	13.712668%
Enzyme redesign $s^\star$	0.110947356	41.605259	10.947356%
$s_{\min}$ with 5% source tolerance	0.119697545	44.886579	19.697545%
Declared parameter box (Appendix B)	0.125895729	47.210898	25.895729%

Table 3: The reconstructed steady state at the attained minimum $s = s_{\min}$, $x = L = X_T$. All four conservation laws and all reaction balances hold; the displayed digits are rounded evaluations, not the exact certificates.

Species	Value (μM)	Species	Value (μM)
NADPH x	0.940319216	Reduced Trx y	0.217306271
NADP^+ $P - x$	29.359680784	Oxidized Trx z_T	0.287693729
Free GSH g	361.118523602	Reduced Prx r	10.000000000
GSSG z	5.219305298	Sulfenic Prx h	0.266666667
Reduced GPx e_0	49.280683581	Hyperoxidized Prx w	0.064000000
Oxidized GPx e_1	0.716450616	Disulfide Prx v	8.765333333
GPx–SSG e_2	0.002865802		

pool of about 9.07×10^4 μM. Even the optimal reallocation still needs more regeneration than the reference setting, $s^\star \approx 0.110947 > 0.1$; that this cannot be evaded by any admitted redesign of the glutathione branch is Proposition 5.2, and it is verified in Lean for the nominal instance.

6.4 Ceilings and the narrow binding interval

The branch ceiling currents of Theorem 4.2 are

$$j_G(N) \approx 10.351642\ \mu\mathrm{M\,s^{-1}}, \qquad j_T(N) \approx 5.143547\ \mu\mathrm{M\,s^{-1}}.$$

Both nominal quotas lie strictly below them, so a finite repair exists; this instance of Theorem 4.2 is verified in Lean. Quotas at or above these values are unattainable at any finite capacity.

Figure 3 shows the resulting quota dependence. Lowering the GPx quota leaves $s_{\min}$ exactly unchanged over the non-binding plateau, while the quota-only line falls, which is the graphical form of Proposition 4.1. The plateau ends at the switching quota $q_G = j_G(X_T) = 10.348944$ $\mu\mathrm{M\,s^{-1}}$, above which the GPx branch binds; the interval between that switch and the ceiling 10.351642 $\mu\mathrm{M\,s^{-1}}$ has width only 0.0027 $\mu\mathrm{M\,s^{-1}}$, which is why it needs an inset rather than a shared axis. Both values must be labelled separately, and neither should be rounded onto the other.

7 How far the criterion extends

Theorem 3.4 uses far less than the specific rate laws of Section 2. This section states what it actually needs, and what replaces it when those hypotheses fail. The results here are conventional mathematics; they are not part of the formalized development.

7.1 Any strictly decreasing source

The proof of Theorem 3.4 uses only that $x \mapsto R_s(x) = s\,r(x)$ is continuous, positive on $[0, N)$, strictly decreasing, and vanishing at N. Hence for any such r,

$$s_{\min} = \frac{J(L)}{r(L)}, \tag{29}$$

with the same necessity, sufficiency and attainment. In particular, multiplying the source by any positive nonincreasing factor preserves the theorem. Product inhibition of the regenerating enzyme by NADPH is of this type: for illustration, $r(x) \mapsto r(x)/(1 + x/K_I)$ is admissible for every $K_I > 0$. We stress that this is a mathematical illustration, not a fitted mechanism for a particular dehydrogenase; a quantitative claim would require the mechanism and assay conditions of the enzyme in question [1, 16].

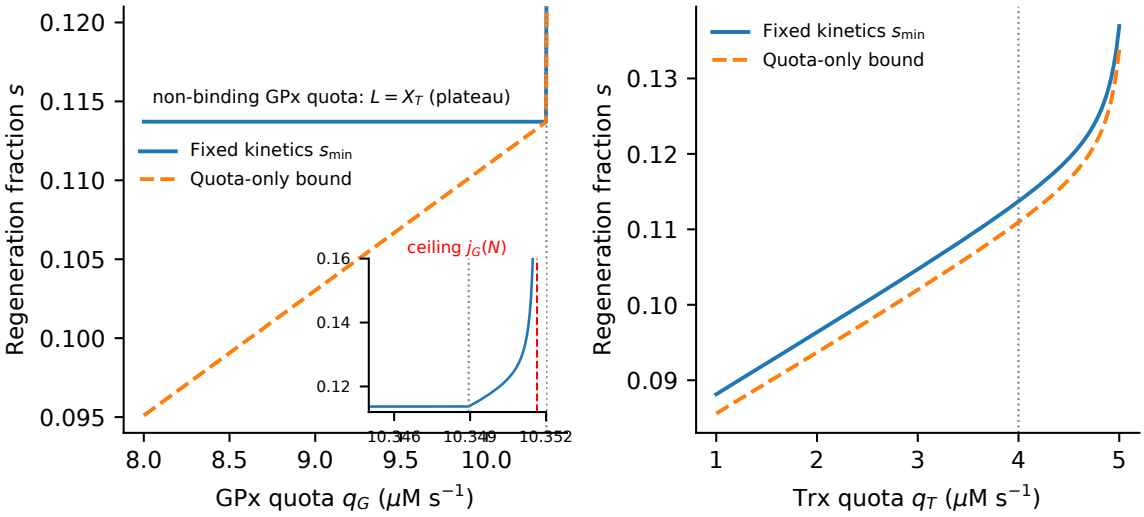

Figure 3: Required regeneration as one quota varies with the other held at its nominal value. Left: over most of the displayed range the GPx quota is non-binding, $L = X_T$, and the fixed-kinetics minimum is exactly constant, while the quota-only bound decreases spuriously; the dotted line marks the switching quota $q_G = j_G(X_T)$, and the inset resolves the narrow interval between that switch and the ceiling $j_G(N)$, where the requirement diverges. Right: raising the Trx quota raises its NADPH floor and hence the requirement. Dashed curves omit kinetic overdelivery.

7.2 More than two branches

For finitely many branches with private states, each with a continuous strictly increasing service current, coupled only through one decreasing source, the proof is unchanged:

$$L = \max_i X_i, \qquad J = \sum_i j_i, \qquad s_{\min} = \frac{J(L)}{r(L)},$$

and the overhead is $\sum_i [j_i(L) - q_i]/r(L)$. This covers additional independent NADPH sinks, but not shared private carriers, competing binding sites, several independent cofactors, or cross-inhibition; those require first reducing the enlarged state equations with the same properties.

7.3 Carrier floors and redox endpoints

Service quotas can be restated in the variables that are actually measured. By (18) the quota $j_i \geq q_i$ is exactly the carrier floor $u_i \geq Y_i$, and conversely a desired free-GSH floor $g \geq g_{\text{req}}$ within the attainable pool range corresponds to

$$q_G = \frac{E_G a_G \, g_{\text{req}}}{g_{\text{req}} + \rho_G}.$$

This is a steady-state equivalence; it does not equate instantaneous oxidative and reductase currents during transients.

Ratio endpoints can be treated the same way, with care about conventions. At fixed temperature Θ, pH and a declared activity convention, the formal half-cell potentials are

$$\mathcal{E}_G = \mathcal{E}_G^{\circ\prime} + \frac{R\Theta}{2F} \ln \frac{a_{\text{GSSG}}}{a_{\text{GSH}}^2}, \qquad \mathcal{E}_T = \mathcal{E}_T^{\circ\prime} + \frac{R\Theta}{2F} \ln \frac{a_{\text{Trx,ox}}}{a_{\text{Trx,red}}}, \tag{30}$$

with dimensionless activities [13]. Inserting bare micromolar numbers into the glutathione logarithm silently changes the standard state and gives an incorrect absolute potential; only $a = c/c^\circ$ with an explicit c° is meaningful. For thioredoxin, $z_T = T - y$, so a specification $\mathcal{E}_T \le \mathcal{E}_{T,\mathrm{target}}$ is equivalent to the carrier floor

$$y \;\ge\; \frac{T}{1+\exp\!\left[2F(\mathcal{E}_{T,\mathrm{target}} - \mathcal{E}_T^{\circ\prime})/(R\Theta)\right]},$$

which enters the same threshold inversion provided it lies in the attainable range. Specifying a favourable potential does not create carrier capacity.

For glutathione, use the *free* g and z, retaining bound material only in the conservation law. At steady state, with $C_0 = E_G a_G / c_G$,

$$z(g) = \tfrac{1}{2}\left(G - g - \frac{C_0}{g+\rho_G}\right), \qquad \frac{\mathrm{d}z}{\mathrm{d}g} = \tfrac{1}{2}\left[-1 + \frac{C_0}{(g+\rho_G)^2}\right],$$

so $C_0 \le \rho_G^2$ is a simple sufficient condition for z to be nonincreasing in g. It holds nominally, with $C_0 = 1.05$ and $\rho_G^2 = 27.783441\ \mu\mathrm{M}^2$. Since g increases with x and $z > 0$, the ratio z/g^2 then strictly decreases, so a feasible upper bound on $\mathcal{E}_G$ also supplies a lower NADPH threshold and can be used in place of a flux quota. This route translates assay specifications into endpoints without importing a generic "healthy potential"; it supplies no standard potentials and no medically meaningful targets, and a Nernst readout does not certify the thermodynamic consistency of an irreversible rate law.

7.4 Non-monotone branch service

Monotonicity of j_i belongs to the mechanism of Section 2. Other mechanisms need not have it: the mechanistic thioredoxin-system model of Pannala and Dash [12] includes NADPH substrate inhibition, which can make a branch current non-monotone in x. Substrate inhibition inside a consuming branch is a different matter from product inhibition of the source, and cannot be handled by (29).

What survives is an exact characterization rather than a threshold. Suppose the private states remain uniquely reconstructible for each x and $r > 0$ on $(0, N)$. Put

$$\mathcal{K} = \{x \in (0,N) :\ j_i(x) \ge q_i \text{ for all } i\}, \qquad h(x) = \frac{J(x)}{r(x)}. \tag{31}$$

Then the set of scales admitting a successful steady state is exactly $\mathcal{S} = h(\mathcal{K})$. For a closed component $[\alpha, \beta]$ of $\mathcal{K}$ on which h is continuous and increasing, the contribution is $[h(\alpha), h(\beta)]$; endpoint inclusion must be handled explicitly for open components. Equivalently, on an interval where F_s is strictly decreasing, a root in $[\alpha, \beta]$ exists exactly when $F_s(\alpha) \ge 0 \ge F_s(\beta)$ — which proves a statement on that interval without excluding roots outside it. Turning this into a decision procedure requires certifying the quota crossings and turning points and bounding h on each monotone piece.

Two conclusions that are sometimes drawn from non-monotonicity do not follow. The first is that the equilibrium must become non-unique; the second is that excess regeneration must be harmless. The following example refutes both simultaneously.

Example 7.1 (Excess regeneration destroys service without bistability). Take the dimensionless system on $0 < x < 1$ with

$$r(x) = 1 - x, \qquad j(x) = x\left(\tfrac{6}{5} - x\right), \qquad q = \tfrac{3}{10}.$$

The current increases up to $x = 3/5$ and decreases thereafter, so it is not monotone. Nevertheless

$$h(x) = \frac{x(6/5 - x)}{1-x}, \qquad h'(x) = \frac{(1-x)^2 + 1/5}{(1-x)^2} > 0,$$

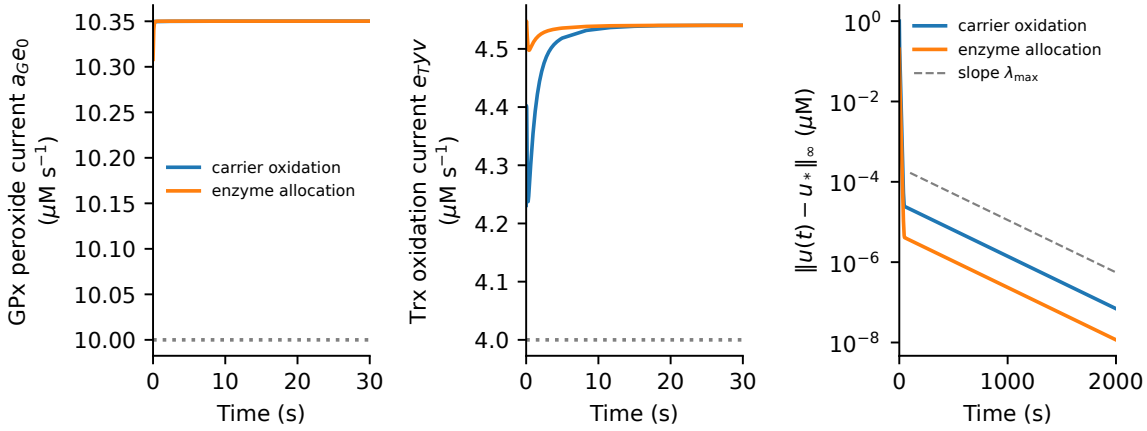

Figure 4: Full-state perturbations at $s = 0.12$, a setting with strict service slack, with initial conditions defined in Appendix A. Left and centre: the peroxide and oxidation currents recover within a few seconds and stay above their quotas (dotted lines) from the first sample. Right: the same trajectories over the full 2000 s integration, measured as the infinity-norm distance to the equilibrium on a logarithmic scale; the grey reference line has the slope of the slowest Jacobian eigenvalue, -0.0030043 s^{-1}. Rapid recovery of the plotted currents and slow relaxation of the full state are different statements.

and h maps $(0, 1)$ onto $(0, \infty)$, so there is exactly one positive equilibrium for every $s > 0$ and no bistability. The quota holds exactly on $\left[\frac{6-\sqrt{6}}{10}, \frac{6+\sqrt{6}}{10}\right]$, equivalently for

$$\frac{12 - 3\sqrt{6}}{10} \;\le\; s \;\le\; \frac{12 + 3\sqrt{6}}{10}, \qquad \text{numerically } 0.465153 \le s \le 1.934847.$$

Thus service has an *upper* operating limit as well as a lower one. In the scalar dynamics $\dot{x} = s\, r(x) - j(x)$ the derivative at equilibrium is $-r(x)h'(x) < 0$, so the example is also locally stable throughout.

Bistability requires multiple stable states and appropriate dynamics; a candidate steady-state fold needs $F_s = 0$ and $\partial F_s/\partial x = 0$ together with a nondegeneracy condition. Non-monotone kinetics alone imply none of this. Note also that monotonicity of each individual branch is sufficient but not necessary for the criterion: what the argument requires is only $F_s' < 0$, which a non-monotone j_i need not violate.

8 Full dynamics: what follows and what does not

After eliminating the four conserved totals, the maintained system has eight independent variables; Appendix A gives the equations, the admitted domain and the numerical protocol.

Forward invariance. The physically admitted closed domain

$$0 \le x \le N, \quad z \ge z_{G0}, \quad z_T \ge z_{T0}, \quad g, e_0, e_1, e_2, y, r, h, w, v \ge 0$$

is forward invariant, by the inward boundary inequalities collected in Appendix A. In particular the baseline-subtracted reductase laws never produce a negative current on this domain, and its compactness excludes finite-time escape. This is a direction-consistency check, not a free-energy realization of the phenomenological model. Neither boundedness nor uniqueness of the equilibrium implies global convergence.

Numerical evidence. At $s = 0.1$, $s = s_{\min}$ and $s = 0.12$ the reconstructed equilibria have residuals below 10^{-12} $\mu\mathrm{M\,s^{-1}}$ and Jacobians whose largest eigenvalue real parts are

$$-0.002999934, \qquad -0.003001207, \qquad -0.003004280 \ \ \mathrm{s^{-1}},$$

so each is numerically locally stable. The corresponding slow modal time scale is about 333 s. Two perturbations were applied at each setting, one oxidizing the carriers and one redistributing enzyme states within their conserved totals. At $s = 0.12$ both trajectories keep both service currents above quota from the first sample; at $s = 0.1$ neither attains joint service; at the exact boundary $s = s_{\min}$, where the limiting service margin is zero, both transiently violate the Trx quota, with sampled minima 3.631856 and 3.944233 $\mu\mathrm{M\,s^{-1}}$, and apparent permanent passage only near 51.55 s. At zero limiting margin such a sampled crossing time is not a certified guarantee, and we do not report it as one. The late-time decay of the full-state error matches the slow eigenvalue to five significant figures (Figure 4, right panel), which is a consistency check on the linearization rather than an independent stability proof.

A monotone-systems shortcut is unavailable. It is tempting to hope that the eight-variable system is cooperative in some orthant order, which would bring the theory of monotone systems to bear [3, 8, 15]. It is not. In the reduced coordinates of Appendix A,

$$\frac{\partial \dot{e}_1}{\partial e_2} = -a_G + b_G e_1, \qquad \frac{\partial \dot{e}_2}{\partial e_1} = b_G g, \tag{32}$$

which at the nominal boundary equilibrium take the values -0.181341975 and 14.444740944 $\mathrm{s^{-1}}$. Their signs are not a floating-point artefact: at steady state $b_G e_1 = j_G/g = a_G e_0/g < a_G$ because $e_0 \le E_G = 50$ while $g > 361$, so the first entry is strictly negative and the second strictly positive. A diagonal sign change $\sigma_i \in \{\pm 1\}$ leaves the product of the two transposed off-diagonal entries unchanged, whereas a cooperative Jacobian would have both nonnegative and hence a nonnegative product. Therefore *no* fixed orthant sign transformation makes this system cooperative near the boundary equilibrium. This does not exclude a more general cone, other coordinates, or a different stability proof; it does exclude treating the standard hypotheses as already satisfied. For the same reason, deficiency-based results [6] cannot be invoked by naming the framework alone: the saturating source and baseline-corrected laws would first have to be given an explicit reaction realization and kinetic class.

What a genuine certificate would require. A local certificate at a point with strict slack, say $s = 0.12$, is the economical next step: enclose the equilibrium with rational bounds keeping strict service margins, rationalize a Lyapunov matrix P for the enclosed linearization, certify $P \succ 0$ and $A^\top P + PA \preceq -\alpha I$, bound the nonlinear remainder by $C\|\xi\|^2$ on an explicit neighbourhood, and choose an ellipsoid on which the cubic term is dominated. A numerical Lyapunov matrix by itself is not that certificate, and none is claimed here. This is optional for a steady-state result and we do not make the present conclusions depend on it.

Because no complete set of reversible rate constants, chemical potentials or chemostat work is specified, a claim of thermodynamic incompatibility would be unsupported, and none is made. Table 4 records what each maintained input is and is not.

9 Relation to existing methods, and a discriminating experiment

Direct numerical solution of the same kinetic model produces the same equilibria. It is a matched computational baseline, not a competing prediction. What the exact analysis adds

Table 4: Maintained-input and material accounting for the declared subsystem.

Feature	Accounting and scope
Peroxide clamp	An external feed balances (7); the challenge is a clamp, not a finite bolus. At the boundary the declared inventory-to-turnover ratio is $H/I_H \approx 7.0 \times 10^{-4}$ s, so the clamp and mixing assumptions need explicit experimental attention.
NADPH regeneration	P is conserved and P_0 is a baseline offset. The product sV scales an externally driven source whose substrate supply and work are not state variables of the model.
Prx maintenance	At the boundary the repair current is $c_T w = b_T j_T / d_T = 0.000192\ \mu\mathrm{M\,s^{-1}}$. It is an external input, not free reducing power, and its ATP and thiol requirements are not resolved [9].
Private inventories	The glutathione total includes GPx-bound material; Trx and both enzyme totals are conserved. The redesign changes only the declared GPx inventory, keeping all carrier totals fixed.
Removed pathways	Protein-thiol reactions, catalase, transport, synthesis and efflux are absent from the selected subsystem. Their protective functions and resource demands cannot be inferred from these results.

is the decision inequality itself, the attainment of the boundary, the impossibility statement below it, uniqueness of the full state, the ceiling equivalence, and the closed-form separation of the three interventions. A simulation alone cannot supply an impossibility certificate.

Thermodynamics-based metabolic flux analysis constrains flux and metabolite activity profiles by thermodynamic feasibility [7]. That addresses a different question from satisfying fixed kinetic branch requirements at one shared concentration in a maintained preparation, and we make no claim to supersede it. Enzyme cost minimization computes enzyme allocations supporting specified fluxes under kinetic and thermodynamic constraints [11]. Our fixed-enzyme theorem holds enzyme pools fixed, while (26) permits exactly one declared design variable and gives a closed-form optimum with a matching lower bound for it; this is narrower than, and not a replacement for, a general allocation framework. Nor is resource competition for NADPH itself a new observation [5, 16]; the contribution here is the exact decision and reconstruction theorem for a declared retained-state model.

A discriminating experiment fixes enzyme amounts, carrier inventories and peroxide conditions, estimates the kinetic parameters and the source response *once* with uncertainty, and then varies regeneration through the precomputed boundary without refitting at each setting. Measurements should resolve NADPH together with branch-resolved turnover or reduced-carrier states, since total NADPH consumption or total peroxide clearance alone does not identify the two branch currents. Useful controls are distinct: removing a branch, relaxing a quota (which is a reporting control only, since it changes no trajectory), and the controlled change of GPx abundance. For the redesign, compare the original and redesigned preparations both at their respective required capacities and at a common capacity, and report service margins and total peroxide turnover separately: an allocation that is optimal for meeting quotas will deliberately reduce turnover above them.

The immediate application setting is a maintained reconstituted or cell-free multienzyme preparation, where independent branch requirements can represent minimum reporter turnover or the preservation of two reduced-carrier pools. This is a proposed application of the model, not a report that such a preparation has been built: the clamp, the baseline-subtracted reductase laws, the conserved pools and the external repair step all still require an implementation or a justified operating approximation. A living-cell interpretation would additionally require transport, alternative clearance, competing NADPH uses, regulation, and justified functional endpoints. Full reproduction of the published cellular time courses and an empirical uncertainty

calibration remain separate tasks, and nothing here is a clinical intervention.

Reproducibility. All constants printed in this paper are recomputed from the model definition by a single replay script, which checks the exact rational thresholds and enclosures, every table entry, the Jacobian spectra, the transient minima and the parameter-box arithmetic. The repository location will be supplied with the author information.

A Full maintained ODE and numerical protocol

Use coordinates $u = (x, z, e_1, e_2, z_T, h, w, v)$ and recover the eliminated variables from the conservation laws,

$$g = G - 2z - e_2, \qquad e_0 = E_G - e_1 - e_2, \qquad y = T - z_T, \qquad r = E_T - h - w - v.$$

Write the glutathione currents as $\Phi_0 = a_G e_0$, $\Phi_1 = b_G g e_1$, $\Phi_2 = c_G g e_2$, $\Psi_G = k_G x(z - z_{G0})$, and the peroxiredoxin–thioredoxin currents as $\Theta_r = a_T r$, $\Theta_w = b_T h$, $\Theta_h = c_T w$, $\Theta_v = d_T h$, $\Theta_y = e_T y v$, $\Psi_T = k_T x(z_T - z_{T0})$. The system is

$$\begin{aligned}(\dot{x}, \dot{z}, \dot{e}_1, \dot{e}_2) &= \big(\, R_s(x) - \Psi_G - \Psi_T,\ \ \Phi_2 - \Psi_G,\ \ \Phi_0 - \Phi_1,\ \ \Phi_1 - \Phi_2 \,\big),\\ (\dot{z}_T, \dot{h}, \dot{w}, \dot{v}) &= \big(\, \Theta_y - \Psi_T,\ \ \Theta_r + \Theta_h - \Theta_w - \Theta_v,\ \ \Theta_w - \Theta_h,\ \ \Theta_v - \Theta_y \,\big).\end{aligned} \tag{33}$$

Forward invariance. On the admitted domain of Section 8 the vector field points inward at every face. At $x = 0$ both reductase currents vanish and $\dot{x} = R_s(0) > 0$; at $x = N$ regeneration vanishes and $\dot{x} = -\Psi_G - \Psi_T \le 0$. At $z = z_{G0}$ and $z_T = z_{T0}$ the derivatives are $\Phi_2 \ge 0$ and $\Theta_y \ge 0$. At $g = 0$ we get $\dot{g} = -\Phi_1 - \Phi_2 + 2\Psi_G = 2\Psi_G \ge 0$, and at $y = 0$, $\dot{y} = \Psi_T \ge 0$. Every zero enzyme state has nonnegative production: in particular $\dot{e}_0 = \Phi_2 - \Phi_0$, $\dot{e}_1 = \Phi_0 - \Phi_1$, $\dot{e}_2 = \Phi_1 - \Phi_2$, $\dot{r} = \Theta_y - \Theta_r$ and $\dot{w} = \Theta_w - \Theta_h$ are nonnegative when the respective variable vanishes. The source denominator stays positive because $D > N$. These inequalities with local smoothness give invariance of the conserved polytope. This is a conventional ODE argument and is not part of the formalized development.

Numerical protocol. Equilibria were located by scalar bracketing of F_s followed by full-state reconstruction through (13)–(14), giving residuals below 10^{-12} $\mu\mathrm{M\,s^{-1}}$. Jacobians were formed by complex-step differentiation with step 10^{-20}, which is free of subtractive cancellation. Integrations used an implicit Radau method with relative tolerance 2×10^{-9} and absolute tolerance 2×10^{-11} over 2000 s, sampled densely over the first 5 s and then every 3.325 s. The carrier-oxidation perturbation increases z by 1 μM and z_T by 0.02 μM; the enzyme-allocation perturbation increases e_1 by 0.2 μM and h by 0.05 μM. Both start strictly inside the admitted domain, and every sampled state remained in it. Final infinity-norm distances to the equilibria were below 1.2×10^{-7} μM.

At $s = 0.12$ the smallest sampled service currents are $(10.349641, 4.231028)$ for carrier oxidation and $(10.308165, 4.497447)$ $\mu\mathrm{M\,s^{-1}}$ for enzyme redistribution, both above quota from the first sample. At $s = s_{\min}$ the respective minimum Trx currents are 3.631856 and 3.944233 $\mu\mathrm{M\,s^{-1}}$, below quota, as discussed in Section 8. Sampling and solver tolerances do not by themselves certify an inequality between samples.

B A conservative declared parameter box

To separate operating tolerance (Section 4.4) from parameter uncertainty, consider an explicit design box in which E_G and E_T vary independently by $\pm 1\%$ and k_G and k_T independently

by ±5%, all other quantities fixed. These intervals are declared assumptions, not estimated biological ranges. All inequalities below are evaluated as exact fractions.

For either branch bound Y_i of (17) by $[Y_i^-, Y_i^+]$. Both nominal coefficients B_i are negative and fixed over this box, so

$$\Delta_i^- = \Gamma_i^- - A_i(Y_i^+)^2 - B_i Y_i^-$$

is a valid lower bound for Δ_i; when it is positive, $X_i \le C_i^+ Y_i^+ / \Delta_i^-$. The glutathione constant uses $\Gamma_G^- = S_G\rho_G - E_G^+ a_G/c_G$, while $\Gamma_T = S_T$ is fixed. This gives

$$X_G < 0.059173\ \mu\text{M}, \qquad X_T < 1.062578\ \mu\text{M}$$

throughout the box. Choose the common target $x_* = 1.5\ \mu$M, which exceeds both. Carrier conservation gives $g \le S_G = 368$ and $y \le S_T = 0.43$, so monotonicity of the rational currents in (12) gives

$$J(x_*) \ \le\ \frac{E_G^+ a_G S_G}{S_G + \rho_G} + \frac{E_T^+ e_T S_T}{1 + \rho_T e_T S_T} \ <\ 15.681942\ \mu\text{M}\,\text{s}^{-1}.$$

Using the exact upper expression, its ratio to $R_1(x_*)$ is the exact rational

$$s_{\text{box}} = \frac{11621793767394811}{92312851976765625} \approx 0.125895729. \tag{34}$$

At this scale the shared residual is nonnegative at x_* for every admitted parameter choice, and negative at N; the decreasing-residual argument then gives a successful equilibrium at or above x_*. Hence s_{box} is sufficient throughout the box. No optimality, corner extremality or empirical confidence is asserted: the bound is deliberately conservative, and it does not assume that the worst case occurs at a corner. If this box and an independent 5% source tolerance are both required, a sufficient command is $s_{\text{box}}/0.95$; the separate rows of Table 2 are not automatically simultaneous guarantees.

C Formal verification: scope and declaration map

C.1 Scope

The central mathematical statements of this paper are machine-checked in Lean 4 [4] against a pinned Mathlib [17], with warnings treated as errors. The authenticated declarations use only the standard axioms `Classical.choice`, `Quot.sound` and `propext`; no admitted theorem, numerical oracle, or native-computation certificate is used for the root theorem, the nominal instance, or the redesign. The root theorem reconstructs literal positive enzyme and carrier states, and does not assume an equilibrium witness.

Formal checking establishes that the stated propositions follow from their stated hypotheses. It does not eliminate the possibility of error in selecting the equations, transcribing the source model, choosing units, or interpreting a theorem biologically. The precise claim is that the listed declarations were kernel checked under their stated assumptions — not that the modelling is thereby validated. Table 5 classifies every substantive claim of the paper by its actual evidence.

C.2 Declaration map

Every name in the table below is to be read inside the single namespace

`CommonEnvironmentProtection`

and the modules are the files of that namespace. The development begins with the quadratic-response and private-branch foundations (`QuadraticPool`, `PrivateBranches`); it adds the monotone-response and maintained-source arguments (`MonotoneResponse`, `MaintainedSource`,

Table 5: Evidence class for each substantive claim.

Claim	Evidence	Location
Private-state elimination and reconstruction	Lean	Prop. 3.1
Continuity, monotonicity, threshold inversion	Lean	Prop. 3.3
Explicit derivative formulas (16)	Conventional	Prop. 3.3
Sharp joint criterion, attainment	Lean	Thm. 3.4
Uniqueness of the full joint steady state	Lean	Thm. 3.5
Separate success, joint failure at s_0	Lean	Sec. 6
Certified enclosure of $s_{\min}$	Lean	Eq. (28)
Overdelivery identity, sign, equality case	Lean	Prop. 4.1
Finite-ceiling equivalence	Lean	Thm. 4.2
Nominal quotas below ceilings	Lean	Sec. 6
Binding-floor identity behind the plateau	Lean	Sec. 4
Regeneration tolerance rule	Lean	Eq. (25)
Redesign attainment and lower bound	Lean	Sec. 5
Reference source insufficient after any redesign	Lean	Sec. 6
Near-ceiling asymptotic cost	Conventional	Cor. 4.3
Sensitivity identities	Conventional	Eq. (24)
Existence of a positive equilibrium below $s_{\min}$	Conventional	Sec. 3.4
General decreasing source, several branches	Conventional	Sec. 7
Carrier-floor and potential translation	Conventional	Sec. 7.3
Interval criterion and Example 7.1	Conventional	Sec. 7.4
Forward invariance of the admitted domain	Conventional	App. A
Orthant-cooperativity obstruction	Conventional	Eq. (32)
Parameter-box sufficiency	Exact rational	App. B
Jacobian spectra, transients, settling	Numerical	Sec. 8

`CoupledPrivate`), the biochemical adapter (`SourceFamilies`), the full-state reconstruction (`LiteralSteady`), the nominal instance (`SourceExample`) and the root file (`Main`). The consequences, the enzyme reallocation and the complements are in `Postproof`, `Allocation` and `Complement`.

Claim	Declaration
Full joint criterion	`jointProtection_iff_minimumRegeneration`
Failure at the reference source	`source_initial_incompatible`
Certified repaired point	`source_certified_repair`
Attained exact minimum	`source_exact_minimum_attained`
Exact rational thresholds	`SourceExample.exact_demand_floors`
Enclosure of $s_{\min}$	`SourceExample.certified_scale_bounds`
Both isolated preparations succeed	`Postproof.isolated_successes`
Current equals quota at its threshold	`Postproof.boundary_flux`
Overdelivery identity	`Postproof.overdelivery_identity`
Overdelivery sign and equality case	`Postproof.overdelivery_nonnegative`
Regeneration tolerance	`Postproof.robust_command`
Binding-quota plateau	`Postproof.binding_floor`
Ceiling obstruction	`Postproof.ceiling_obstruction`
Redesign attainment	`Allocation.allocation_attained`
Redesign universal lower bound	`Allocation.allocation_lower_bound`
Reference source insufficient after redesign	`Allocation.original_source_insufficient_for_redesign`
Quota below ceiling admits inversion	`Complement.ceiling_admits`
Finite-repair equivalence	`Complement.finite_repair_iff`
Uniqueness of the full joint state	`Complement.joint_state_unique`
Nominal quotas below both ceilings	`Complement.nominal_quotas_below_ceilings`

The exact types, hypotheses and imported axioms of these declarations, not their names, are the authority for what has been checked. Three strict verification receipts record the compiler invocation, the source and dependency hashes, the exported declaration interfaces and the axiom list. The claims listed as conventional or numerical in Table 5 are proved or computed in this manuscript and are deliberately not attributed to those receipts.

References

[1] S. A. Adediran. Kinetic properties of normal human erythrocyte glucose-6-phosphate dehydrogenase dimers. *Biochimie*, 73(9):1211–1218, 1991. doi: 10.1016/0300-9084(91)90006-M.

[2] Nkechi J. Adimora, Dean P. Jones, and Melissa L. Kemp. A model of redox kinetics implicates the thiol proteome in cellular hydrogen peroxide responses. *Antioxidants & Redox Signaling*, 13(6): 731–743, 2010. doi: 10.1089/ars.2009.2968.

[3] David Angeli and Eduardo D. Sontag. Monotone control systems. *IEEE Transactions on Automatic Control*, 48(10):1684–1698, 2003. doi: 10.1109/TAC.2003.817920.

[4] Leonardo de Moura and Sebastian Ullrich. The Lean 4 theorem prover and programming language. In *Automated Deduction – CADE 28*, volume 12699 of *Lecture Notes in Computer Science*, pages 625–635, 2021. doi: 10.1007/978-3-030-79876-5_37.

[5] Jing Fan, Jiangbin Ye, Jurre J. Kamphorst, Tomer Shlomi, Craig B. Thompson, and Joshua D. Rabinowitz. Quantitative flux analysis reveals folate-dependent NADPH production. *Nature*, 510 (7504):298–302, 2014. doi: 10.1038/nature13236.

[6] Martin Feinberg. Chemical reaction network structure and the stability of complex isothermal reactors I: the deficiency zero and deficiency one theorems. *Chemical Engineering Science*, 42(10): 2229–2268, 1987. doi: 10.1016/0009-2509(87)80099-4.

[7] Christopher S. Henry, Linda J. Broadbelt, and Vassily Hatzimanikatis. Thermodynamics-based metabolic flux analysis. *Biophysical Journal*, 92(5):1792–1805, 2007. doi: 10.1529/biophysj.106.093138.

[8] Morris W. Hirsch. Systems of differential equations that are competitive or cooperative II: convergence almost everywhere. *SIAM Journal on Mathematical Analysis*, 16(3):423–439, 1985. doi: 10.1137/0516030.

[9] Thomas J. Jönsson, Michael S. Murray, Lynnette C. Johnson, and W. Todd Lowther. Reduction of cysteine sulfinic acid in peroxiredoxin by sulfiredoxin proceeds directly through a sulfinic phosphoryl ester intermediate. *Journal of Biological Chemistry*, 283(35):23846–23851, 2008. PMCID: PMC2527103.

[10] Jun Lu and Arne Holmgren. The thioredoxin antioxidant system. *Free Radical Biology and Medicine*, 66:75–87, 2014. doi: 10.1016/j.freeradbiomed.2013.07.036.

[11] Elad Noor, Avi Flamholz, Arren Bar-Even, Dan Davidi, Ron Milo, and Wolfram Liebermeister. The protein cost of metabolic fluxes: prediction from enzymatic rate laws and cost minimization. *PLOS Computational Biology*, 12(11):e1005167, 2016. doi: 10.1371/journal.pcbi.1005167.

[12] Venkat R. Pannala and Ranjan K. Dash. Mechanistic characterization of the thioredoxin system in the removal of hydrogen peroxide. *Free Radical Biology and Medicine*, 78:42–55, 2015. doi: 10.1016/j.freeradbiomed.2014.10.508.

[13] Freya Q. Schafer and Garry R. Buettner. Redox environment of the cell as viewed through the redox state of the glutathione disulfide/glutathione couple. *Free Radical Biology and Medicine*, 30 (11):1191–1212, 2001. doi: 10.1016/S0891-5849(01)00480-4.

[14] Helmut Sies. Hydrogen peroxide as a central redox signaling molecule in physiological oxidative stress: oxidative eustress. *Redox Biology*, 11:613–619, 2017. doi: 10.1016/j.redox.2016.12.035.

[15] Hal L. Smith. *Monotone Dynamical Systems: An Introduction to the Theory of Competitive and Cooperative Systems*, volume 41 of *Mathematical Surveys and Monographs*. American Mathematical Society, 1995.

[16] Robert C. Stanton. Glucose-6-phosphate dehydrogenase, NADPH, and cell survival. *IUBMB Life*, 64(5):362–369, 2012. doi: 10.1002/iub.1017.

[17] The mathlib Community. The Lean mathematical library. Proceedings of the 9th ACM SIGPLAN International Conference on Certified Programs and Proofs (CPP 2020), 367–381, 2020.

[18] Christine C. Winterbourn and Mark B. Hampton. Thiol chemistry and specificity in redox signaling. *Free Radical Biology and Medicine*, 45(5):549–561, 2008. doi: 10.1016/j.freeradbiomed.2008.05.004.